Quasi-monochromatic polycapillary imaging utilizing a computed radiography system

Eiichi Sato[a], Yasuomi Hayasi[a], Etsuro Tanaka[b], Hidezo Mori[c], Toshiaki Kawai[d], Toshio Ichimaru[e], Fumiko Obata[f], Kiyomi Takahashi[f], Sigehiro Sato[f], Kazuyoshi Takayama[g] and Hideaki Ido[h]

[a]Department of Physics, Iwate Medical University, 3-16-1 Honchodori, Morioka 020-0015, Japan
[b]Department of Nutritional Science, Faculty of Applied Bio-science, Tokyo University of Agriculture, 1-1-1 Sakuragaoka, Setagaya-ku 156-8502, Japan
[c]Department of Cardiac Physiology, National Cardiovascular Center Research Institute, 5-7-1 Fujishiro-dai, Suita, Osaka 565-8565, Japan
[d]Electron Tube Division #2, Hamamatsu Photonics Inc., 314-5 Shimokanzo, Toyooka Village, Iwata-gun 438-0193, Japan
[e]Department of Radiological Technology, School of Health Sciences, Hirosaki University, 66-1 Honcho, Hirosaki 036-8564, Japan
[f]Department of Microbiology, School of Medicine, Iwate Medical University, 19-1 Uchimaru, Morioka 020-8505, Japan
[g]Shock Wave Research Center, Institute of Fluid Science, Tohoku University, 2-1-1 Katahira, Aoba-ku, Sendai 980-8577, Japan
[h]Department of Applied Physics, Faculty of Engineering, Tohoku Gakuin University, 1-13-1 Chuo, Tagajo 985-8537, Japan

ABSTRACT

A fundamental study on quasi-monochromatic parallel radiography using a polycapillary plate and a copper-target x-ray tube is described. The x-ray generator consists of a negative high-voltage power supply, a filament (hot cathode) power supply, and an x-ray tube. The negative high-voltage is applied to the cathode electrode, and the anode electrode is connected to the ground. In this experiment, the tube voltage was regulated from 12 to 22 kV, and the tube current was regulated within 3.0 mA by the filament temperature. The exposure time was controlled in order to obtain optimum x-ray intensity, and the maximum focal spot dimensions were approximately 2.0×1.5 mm. The polycapillary plate was J5022-16 (Hamamatsu Photonics Inc.), and the plate thickness was 1.0 mm. The outer, effective, and hole diameters were 33 mm, 27 mm, and 10 µm, respectively. Quasi-monochromatic x-rays were produced using a 10 µm-thick copper filter with a tube voltage of 17 kV, and these rays were formed into parallel beams by the polycapillary. The radiogram was taken using a computed radiography system utilizing imaging plates. In the measurement of image resolution, the resolution hardly varied according to increases in the distance between the chart and imaging plate using a polycapillary. We could observe a 50 µm tungsten wire clearly, and fine blood vessels of approximately 100 µm were visible in angiography.

Keywords: Parallel radiography, quasi-monochromatic x-ray, characteristic x-ray, x-ray lens, polycapillary plate

1. INTRODUCTION

Monochromatic parallel x-ray beams are typically produced by a synchrotron in conjunction with single crystals and have been applied in high contrast micro-angiography[1] and x-ray phase imaging.[2-4] In order to produce quasi-monochromatic x-rays without using the synchrotron, we developed a transmission type molybdenum x-ray tube.[5] Subsequently, flash x-ray tubes are employed to primarily perform high speed radiographies with biomedical applications. In particular, plasma flash x-ray tubes are very useful to produce intense and sharp characteristic x-rays[6-11] such as lasers.

With recent advances in x-ray optics, several different x-ray lenses[12,13] have been developed, and a polycapillary plate[5,8,14] has been shown to be useful to realize a low-priced x-ray system and to perform parallel radiography. Therefore, we performed parallel radiography using a tungsten-target x-ray tube and an x-ray film because the film is conventional and is useful to obtain a high image resolution.

In biomedical radiography, because both the brightness and the contrast of radiograms can be controlled by a Computed Radiography (CR) system[15] utilizing imaging plates, the CR system is useful to perform quasi-monochromatic parallel radiography, regardless of whether the image resolution falls. Therefore, in conjunction with the CR, we have to measure the fundamental characteristics of the polycapillary radiography.

In this paper, we describe a quasi-monochromatic parallel radiography system utilizing a fine polycapillary plate with a hole diameter of 10 μm, a CR system, and a copper-target radiation tube in order to create a conventional x-ray system to be used instead of the synchrotron.

2. EXPERIMENTAL SETUP

Figure 1 shows the circuit diagram of the x-ray generator, which consists of a negative high-voltage power supply, a filament (hot cathode) power supply, and a copper-target x-ray tube. The negative high-voltage is applied to the cathode electrode, and the anode (target) is connected to the ground. In this experiment, the tube voltage was regulated from 12 to 22 kV, and the tube current was regulated by the filament temperature and ranged from 1.0 to 3.0 mA. The exposure time was controlled in order to obtain optimum x-ray intensity.

The experimental setup for performing parallel radiography is shown in Fig. 2. Quasi-monochromatic x-rays are produced using a 10 μm-thick copper filter, and these rays are formed into parallel beams by a polycapillary plate (Fig. 3). The polycapillary is J5022-16 (Hamamatsu Photonics Inc.), and the thickness and the hole diameter of the polycapillary are 1.0 mm and 10 μm, respectively. Radiography was performed by a CR system (Konica Regius 150) utilizing imaging plates.

The distance between the x-ray source and the polycapillary was 1.08 m, and the polycapillary plate was set on the aluminum plate. The distance between the polycapillary and imaging plates was regulated by the height of polymethyl methacrylate (PMMA) spacers of 30 mm in height. At a constant distance between the polycapillary and the imaging plate, the distance between the imaging plate and the chart was regulated by pipe-shaped brass spacers of 30 and 60 mm in height.
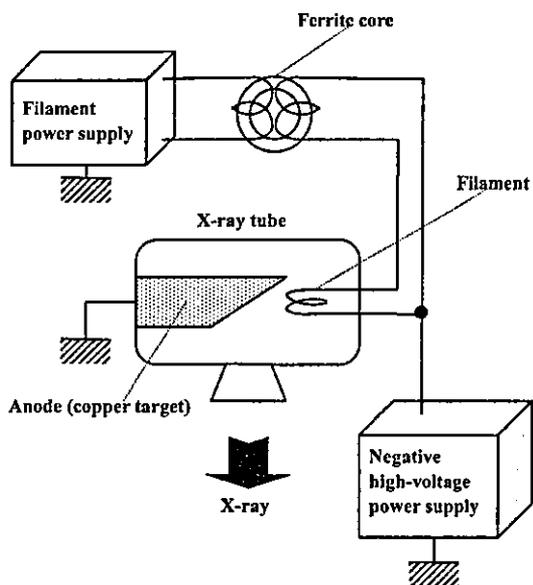
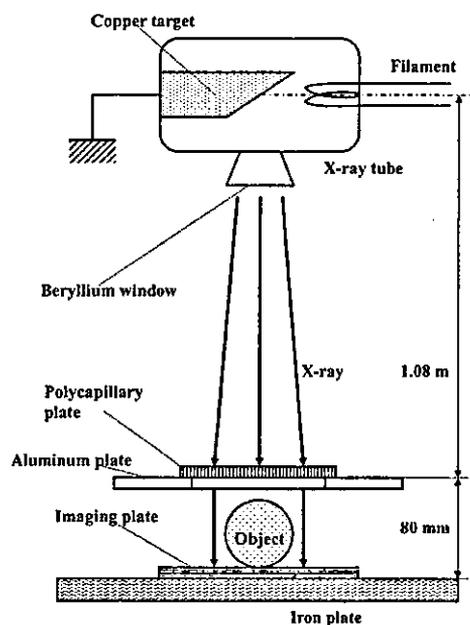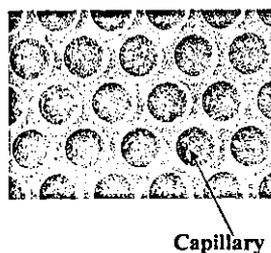Figure 1: Circuit diagram of the x-ray generator.

Figure 2: Experimental setup for parallel radiography utilizing a polycapillary plate and a CR system.

Capillary

Figure 3: Polycapillary plate.

3. CHARACTERISTICS

3.1 Focal spot

In order to measure images of the x-ray source, we employed a pinhole camera with a hole diameter of 50 μm (Fig. 4). When the tube voltage was increased, the spot intensity increased, and spot dimensions increased slightly and had values of approximately 2.0×1.5 mm.

3.2 X-ray spectra

X-ray spectra from the copper-target tube were measured by a transmission-type spectrometer with a lithium fluoride curved crystal 0.5 mm in thickness (Fig. 5). The spectra were taken by the CR system with a wide dynamic range, and relative x-ray intensity was calculated from Dicom digital data. Figure 6 shows measured spectra from the

copper target. When the tube voltage was increased, the bremsstrahlung x-ray intensity increased, and the characteristic x-ray intensity of K_α and K_β lines also increased. Following insertion of the copper filter, the bremsstrahlung x-rays with energies higher than the K-absorption edge were absorbed effectively.
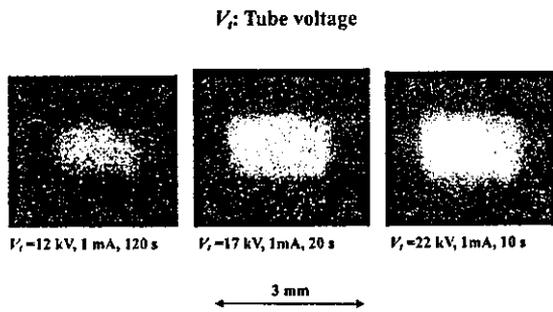
V_t: Tube voltage

V_t=12 kV, 1 mA, 120 s V_t=17 kV, 1mA, 20 s V_t=22 kV, 1mA, 10 s

3 mm

Figure 4: Images of the x-ray source measured by a 50 µm-diameter pinhole with changes in the tube voltage.
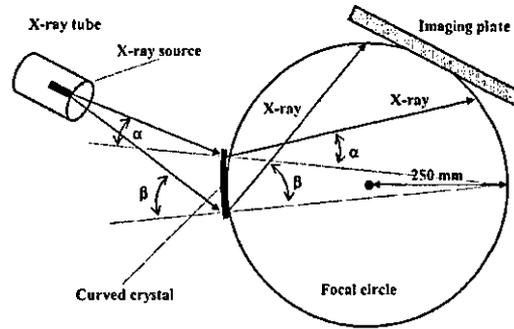

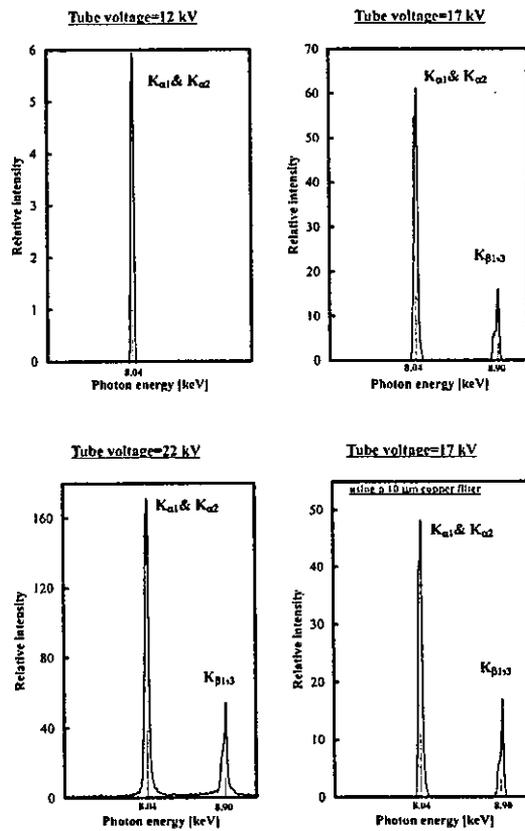Figure 5: Transmission-type spectrometer with a lithium fluoride curved crystal and an imaging plate.

Figure 6: Measured x-ray spectra according to changes in the tube voltage.

4. RADIOGRAPHY

The quasi-monochromatic radiography was performed with a tube voltage of 17 kV using the filter. Figure 7 shows radiography for imaging a polycapillary plate, and the radiograms of the polycapillary are shown in Fig. 8. The center of the black spot in the polycapillary radiogram was mainly imaged by direct transmission beams through capillary holes. As shown in this figure, the spot dimensions increased slightly according to decreases in the PMMA spacer height.

Figure 9 shows the parallel radiography for imaging a test chart, and the polycapillary was set on the aluminum plate. In this radiography, when the spacer height was increased, the image resolution hardly varied, and the image dimensions decreased slightly (Fig. 10). Next, when the height of the brass spacer was decreased, the image resolution hardly varied, and the dimensions again decreased slightly (Figs. 11 and 12).

Figures 13 and 14 show radiography and the radiogram of tungsten wires on a PMMA spacer, respectively. Although the image contrast increased with increases in the wire diameter, a 50 μm-diameter wire could be observed. An angiography of a rabbit heart is shown in Fig. 15; iodine-based microspheres of 20 μm diameter were used, and fine blood vessels of about 50 μm were visible (Fig. 16).
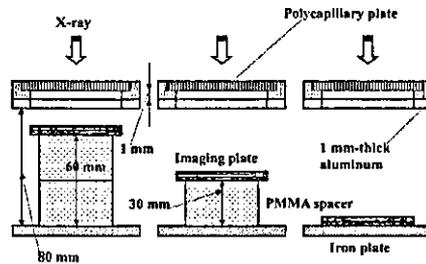

Figure 7: Radiography for imaging a polycapillary plate according to changes in the distance between the polycapillary and imaging plates.

H_p: PMMA spacer height

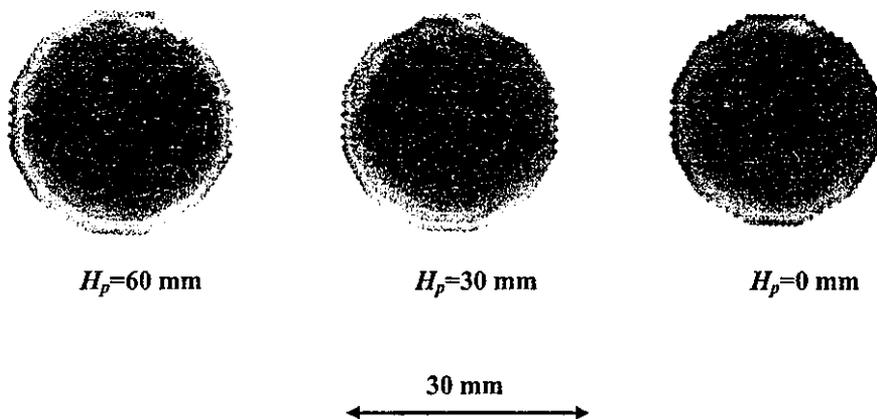H_p=60 mm H_p=30 mm H_p=0 mm

30 mm

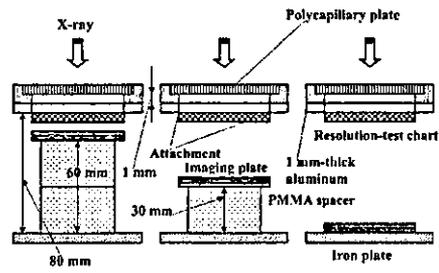Figure 8: Radiograms of a polycapillary plate according to changes in the PMMA height.

Figure 9: Radiography for imaging a test chart using a polycapillary plate according to the PMMA height.

H_p: PMMA spacer height

100 μm

125 μm

166 μm

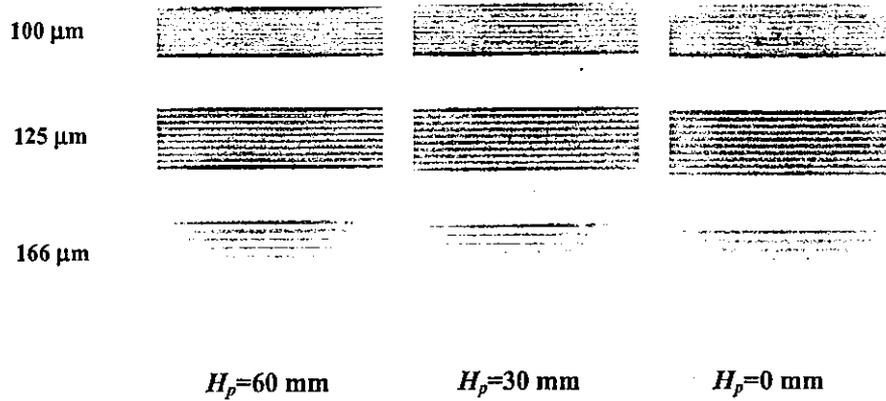H_p=60 mm H_p=30 mm H_p=0 mm

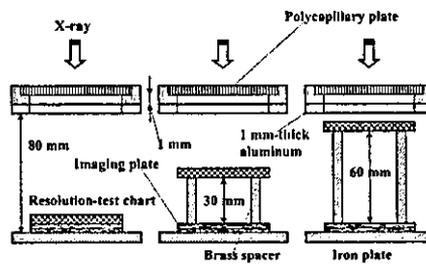Figure 10: Radiograms of a test chart using a polycapillary plate according to the PMMA height.

Figure 11: Radiography for imaging a test chart using a polycapillary plate according to the brass spacer height.

H_b: Brass spacer height

100 μm		
125 μm		
166 μm		

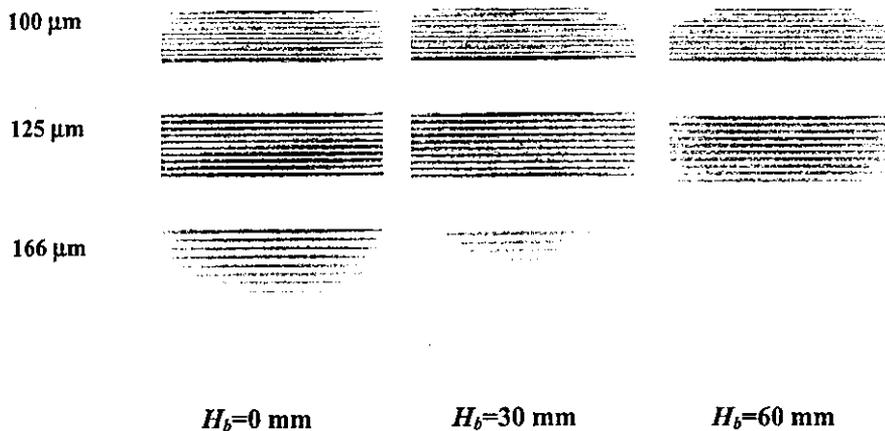H_b=0 mm H_b=30 mm H_b=60 mm

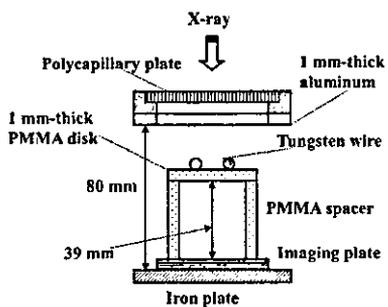Figure 12: Radiograms of a test chart using the polycapillary according to the brass spacer height.

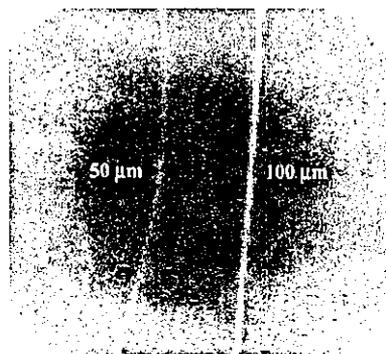Figure 13: Radiography for imaging tungsten wires using the polycapillary.

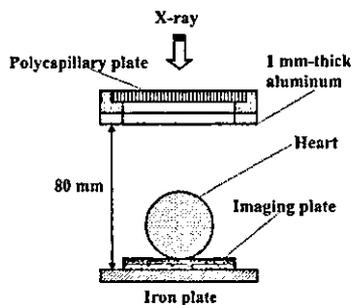Figure 14: Radiograms of tungsten wires on a PMMA spacer.

Figure 15: Parallel angiography of a heart extracted from a rabbit using iodine-based microspheres.
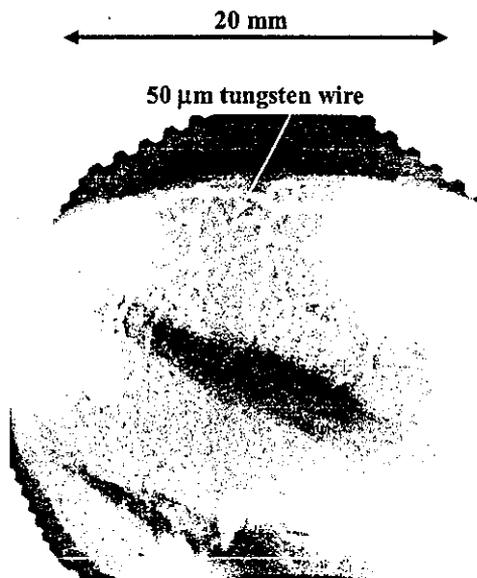
Figure 16: Angiogram of the heart using the polycapillary.

5. DISCUSSION

In this research, we performed parallel radiography achieved with a polycapillary plate in conjunction with quasi-monochromatic x-rays, and obtained slightly higher image resolutions as compared with those obtained without using the plate. Currently, the image resolution of the polycapillary is primarily determined by the diameter of the capillary hole and the thickness, and is improved with decreases in the diameter and increases in the thickness. In cases where the CR system is employed, although the resolution of the CR system is primarily determined by the minimum sampling pitch of 87.5 μm, we could observe 50 μm tungsten wires easily.

The photon energies of the characteristic x-rays are determined by the target element, and the capillary thickness should be increased according to increases in the photon energy because the transmission intensity through capillary glass increases. Subsequently, in order to increase the parallelity for phase imaging, single crystals should be employed after passing through the polycapillary.

Because it is possible to increase the irradiation field by increasing the distance between the x-ray source and the polycapillary, this system can be applied to image a wide variety of objects in various fields, including medical radiography.

ACKNOWLEDGMENTS

REFERENCES

1. H. Mori, K. Hyodo, E. Tanaka, M.U. Mohammed, A. Yamakawa, Y. Shinozaki, H. Nakazawa, Y. Tanaka, T. Sekka, Y. Iwata, S. Honda, K. Umetani, H. Ueki, T. Yokoyama, K. Tanioka, M. Kubota, H. Hosaka, N. Ishizawa and M. Ando, "Small-vessel radiography in situ with monochromatic synchrotoron radiation," *Radiology*, **201**, pp. 173-177, 1996.

2. T.J. Davis, D. Gao, T.E. Gureyev, A.W. Stevenson and S.W. Wilkims, "Phase-contrast imagimg of weakly absorbing materials using hard x-rays," *Nature*, **373**, pp. 595-597, 1995.

3. A. Momose, T. Takeda, Y. Itai and K. Hirano, "Phase-contrast x-ray computed tomography for observing biological soft tissues," *Nature Medicine*, **2**(4), pp. 473-475, 1996.

4. A. Ishisaka, H. Ohara and C. Honda, "A new method of analyzing edge effect in phase contrast imaging with incoherent x-rays," *Opt. Rev*, **7**, pp. 566-572, 2000.

5. E. Sato, M. Komatsu, Y. Hayasi, E. Tanaka, H. Mori, T. Kawai, T. Usuki, K. Sato, T. Ichimaru, K. Takayama and H. Ido, "Quasi-monochromatic parallel radiography achieved with a plane-focus x-ray tube," *SPIE*, **4786**, pp. 151-161. 2002.

6. E. Sato, Y. Hayasi, H. Mori, E. Tanaka, K. Takayama, H. Ido, K. Sakamaki and Y. Tamakawa, "Quasi-monochromatic x-ray production from the cerium target," *SPIE*, **4142**, pp. 17-28, 2000.

7. E. Sato, Y. Suzuki, Y. Hayashi, E. Tanaka, H. Mori, T. Kawai, K. Takayama, H. Ido and Y. Tamakawa, "High-intensity quasi-monochromatic x-ray irradiation from the linear plasma target," *SPIE*, **4505**, pp. 154-164, 2001.

8. E. Sato, Y. Hayashi, E. Tanaka, H. Mori, T. Kawai, H. Obara, T. Ichimaru, K. Takayama, H. Ido, T. Usuki, K. Sato and Y. Tamakawa, "Polycapillary radiography using a quasi-x-ray laser generator," *SPIE*, **4508**, pp. 176-187, 2001.

9. E. Sato, Y. Hayasi, E. Tanaka, H. Mori, T. Kawai, T. Usuki, K. Sato, H. Obara, T. Ichimaru, K. Takayama, H. Ido and Y. Tamakawa, "Quasi-monochromatic radiography using a high-intensity quasi-x-ray laser generator," *SPIE*, **4682**, pp. 538-548 2002.

10. E. Sato, Y. Hayasi, E. Tanaka, H. Mori, T. Kawai, K. Takayama and H. Ido, "Irradiation of intense characteristic x-rays from weakly ionized linear plasma," *Proc 3rd Korea-Japan Joint Meeting on Medical Physics, Gyeongju*, pp. 396-399, 2002.

11. E. Sato, Y. Hayasi, R. Germer, E. Tanaka, H. Mori, T. Kawai, H. Obara, T. Ichimaru, K. Takayama and H. Ido, "Intense characteristic x-ray irradiation from weakly ionized linear plasma and applications," *Jpn. J. Med. Imag. Inform. Sci.*, **20**, pp. 148-155. 2003.

12. Q.F. Xiao and S.V. Poturaef, "Polycapillary-based x-ray optics," *Nucl. Instr. Meth. Phys. Res. A*, **347**, pp. 376-383, 1994.

13. A.A. Bzhanmikov, N. Langhoff, J. Schmalz, R. Wedell, V.L. Beloglazov and N.F. Lebedev, "Polycapillary conic collimator for micro-XRF," *SPIE*, **3444**, pp. 430-435, 1998.

14. E. Sato, H. Toriyabe, Y. Hayasi, E. Tanaka, H. Mori, T. Kawai, T. Usuki, K. Sato, H. Obara, T. Ichimaru, K. Takayama, H. Ido and Y. Tamakawa, "Fundamental study on parallel beam radiography using a polycapillary plate," *SPIE*, **4682**, pp. 298-310, 2002.

15. E. Sato, K. Sato and Y. Tamakawa, "Film-less computed radiography system for high-speed Imaging," *Ann. Rep. Iwate Med. Univ. Sch. Lib. Arts and Sci.*, **35**, pp. 13-23, 2000.

Effects of Adrenomedullin Inhalation on Hemodynamics and Exercise Capacity in Patients With Idiopathic Pulmonary Arterial Hypertension

Noritoshi Nagaya, MD; Shingo Kyotani, MD; Masaaki Uematsu, MD; Kazuyuki Ueno, PhD; Hideo Oya, MD; Norifumi Nakanishi, MD; Mikiyasu Shirai, MD; Hidezo Mori, MD; Kunio Miyatake, MD; Kenji Kangawa, PhD

Background—Adrenomedullin (AM) is a potent pulmonary vasodilator peptide. However, whether intratracheal delivery of aerosolized AM has beneficial effects in patients with idiopathic pulmonary arterial hypertension remains unknown. Accordingly, we investigated the effects of AM inhalation on pulmonary hemodynamics and exercise capacity in patients with idiopathic pulmonary arterial hypertension.

Methods and Results—Acute hemodynamic responses to inhalation of aerosolized AM ($10~\mu g/kg$ body wt) were examined in 11 patients with idiopathic pulmonary arterial hypertension during cardiac catheterization. Cardiopulmonary exercise testing was performed immediately after inhalation of aerosolized AM or placebo. The work rate was increased by 15 W/min until the symptom-limited maximum, with breath-by-breath gas analysis. Inhalation of AM produced a 13% decrease in mean pulmonary arterial pressure (54 ± 3 to 47 ± 3 mm Hg, $P<0.05$) and a 22% decrease in pulmonary vascular resistance (12.6 ± 1.5 to 9.8 ± 1.3 Wood units, $P<0.05$). However, neither systemic arterial pressure nor heart rate was altered. Inhalation of AM significantly increased peak oxygen consumption during exercise (peak $\dot{V}O_2$, 14.6 ± 0.6 to 15.7 ± 0.6 mL $\cdot$ kg^{-1} $\cdot$ min^{-1}, $P<0.05$) and the ratio of change in oxygen uptake to that in work rate ($\Delta\dot{V}O_2/\Delta W$ ratio, 6.3 ± 0.4 to 7.0 ± 0.5 mL $\cdot$ min^{-1} $\cdot$ W^{-1}, $P<0.05$). These parameters remained unchanged during placebo inhalation.

Conclusions—Inhalation of AM may have beneficial effects on pulmonary hemodynamics and exercise capacity in patients with idiopathic pulmonary arterial hypertension. (*Circulation*. 2004;109:351-356.)

Key Words: peptides ■ hypertension, pulmonary ■ respiration ■ exercise ■ hemodynamics

Idiopathic pulmonary arterial hypertension is a rare but life-threatening disease characterized by progressive pulmonary hypertension, ultimately producing right heart failure and death.[1] Although a variety of vasodilators have been proposed as potential therapy for this disease over the past 30 years,[2,3] some patients ultimately require heart-lung or lung transplantation.[8,9] Thus, a novel therapeutic strategy is desirable.

Adrenomedullin (AM) is a potent, long-lasting vasodilator peptide that was originally isolated from human pheochromocytoma.[10] Immunoreactive AM has subsequently been detected in plasma and a variety of tissues, including blood vessels and lungs.[11,12] It has been reported that there are abundant binding sites for AM in the lungs.[13] We have shown that the plasma AM level increases in proportion to the severity of pulmonary hypertension and that circulating AM is partially metabolized in the lungs.[14,15] Interestingly, AM

has been shown to inhibit the migration and proliferation of vascular smooth muscle cells.[16,17] These findings suggest that AM plays an important role in the regulation of pulmonary vascular tone and vascular remodeling. In fact, we have shown that short-term intravenous infusion of AM significantly decreases pulmonary vascular resistance in patients with congestive heart failure[18] or pulmonary arterial hypertension.[19] Unfortunately, however, intravenously administered AM induced systemic hypotension in such patients because of nonselective vasodilation in the pulmonary and systemic vascular beds.

More recently, inhalation of aerosolized prostacyclin and its analogue iloprost has been shown to cause pulmonary vasodilation without systemic hypotension in patients with idiopathic pulmonary arterial hypertension.[20,21] In addition, inhalant application of vasodilators does not impair gas exchange because the ventilation-matched deposition of drug

351

TABLE 1. Baseline Characteristics of Patients With Idiopathic Pulmonary Arterial Hypertension

Demographics	
Age. y	39 ± 3
Male/female. n	2/9
NYHA functional class. n	
III	10
IV	1
Baseline hemodynamics	
MPAP, mm Hg	54 ± 3
CI, L · min^{-1} · m^{-2}	2.4 ± 0.1
PVR. Wood units	12.6 ± 1.5
RAP, mm Hg	7 ± 1
PCWP. mm Hg	7 ± 1
Pulmonary function	
Sa$_{O_2}$. %	94 ± 3
Svo$_2$. %	63 ± 4
FVC, % predicted	86 ± 4
FEV$_1$, % predicted	75 ± 1
6-Minute walk test, m	355 ± 35
Medication use, n	
Anticoagulant agents	10
Diuretics	9
Digitalis	7
Oral prostacyclin analogue	6
Calcium antagonists	2

NYHA indicates New York Heart Association; MPAP, mean pulmonary arterial pressure; CI. cardiac index; PVR. pulmonary vascular resistance; RAP, mean right atrial pressure; PCWP, pulmonary capillary wedge pressure; Sa$_{O_2}$. arterial oxygen pressure; Svo$_2$. mixed venous oxygen saturation; FVC, forced vital capacity; and FEV$_1$, forced expiratory volume in 1 second. Data are mean ± SEM.

in the alveoli causes pulmonary vasodilation matched to ventilated areas.[20] In clinical settings, inhalation therapy may be more simple, noninvasive, and comfortable than continuous intravenous infusion therapy. Thus, the purpose of the present study was to investigate the effects of AM inhalation on hemodynamics and exercise capacity in patients with idiopathic pulmonary arterial hypertension.

Methods

Study Subjects

Eleven patients with idiopathic pulmonary arterial hypertension (9 women and 2 men; age, 39 ± 3 years) were included in this study. Idiopathic pulmonary arterial hypertension was defined as pulmonary hypertension unexplained by any secondary cause, on the basis of the criteria of the National Institutes of Health registry.[1] Ten patients were classified as New York Heart Association (NYHA) functional class III and 1 as class IV (Table 1). Two of the 11 patients (18%) were acute responders who showed a significant decrease in mean pulmonary arterial pressure of >20% with a decrease in mean pulmonary arterial pressure to <35 mm Hg and no change or an increase in cardiac index during short-term infusion of epoprostenol. Long-term medication, including anticoagulant agents, digitalis. and diuretics, was kept constant. Vasodilator agents, such as oral prostacyclin analogue and calcium antagonists, were stopped >12 hours before the study procedure was begun. The ethics

committee of the National Cardiovascular Center approved the study, and all patients gave written informed consent.

Preparation of Human AM

Human AM was dissolved in saline with 4% D-mannitol and sterilized by passage through a 0.22-μm filter (Millipore Co). At the time of dispensing. randomly selected vials were submitted for sterility and pyrogen testing. The chemical nature and content of the human AM in vials were verified by high-performance liquid chromatography and radioimmunoassay. All vials were stored frozen at -80°C from the time of dispensing until the time of preparation for administration.

Hemodynamic Studies

Acute hemodynamic responses to AM inhalation were assessed in all patients while they were in a stable condition during hospitalization. Hemodynamic variables. including pulmonary arterial pressure, right atrial pressure. pulmonary capillary wedge pressure. and cardiac output (in triplicate). were determined with a thermodilution catheter (TOO211I-7.5F. Baxter Co).[22] A 22-gauge cannula was inserted into a radial artery for hemodynamic measurements and blood sampling. After an equilibration period of 30 minutes. baseline hemodynamics were measured. Then. AM (10 μg/kg body wt) was inhaled as an aerosol with a jet nebulizer (Porta-Nebu. MEDIC-AID) for 15 minutes. which resulted in a cumulative dose of 400 to 600 μg AM. Hemodynamic parameters were measured at 15-minute intervals starting 15 minutes before AM inhalation until 60 minutes after inhalation. Blood samples for AM measurement were taken at 15-minute intervals from 15 minutes before inhalation until 60 minutes after the end of inhalation.

Cardiopulmonary Exercise Testing

The effects of AM inhalation on exercise capacity were examined in 10 of 11 patients; 1 patient with NYHA class IV underwent the 6-minute walk test according to decision of attending physicians. Cardiopulmonary exercise testing was performed immediately after inhalation of aerosolized AM (10 μg/kg body wt) or saline in a double-blind. randomized. crossover design. This study was performed on 2 separate days. 1 week apart. The first cardiopulmonary exercise testing was performed within 10 days after the cardiac catheterization. The patients performed exercise seated on a cycle ergometer. They first pedaled at 55 rpm without any added load for 1 minute. The work rate was then increased by 15 W/min up to the symptom-limited maximum. Breath-by-breath gas analysis was performed with an AE280 (Minato Medical Science) connected to a personal computer running analyzing software.[23] The ratio of change in oxygen uptake to that in work rate ($\Delta \dot{V}o_2/\Delta W$ ratio) was calculated as the slope of oxygen consumption per unit workload from 1 minute after the start of load addition until 85% maximal $\dot{V}o_2$. Exercise capacity was evaluated by peak oxygen consumption (peak $\dot{V}o_2$). which was defined as the value of averaged data during the final 15 seconds of exercise. Ventilatory efficiency during exercise was represented by the $\dot{V}E$-$\dot{V}co_2$ slope, which was determined as the linear regression slope of $\dot{V}E$ and $\dot{V}co_2$ from the start of exercise until the RC point (the time until which ventilation is stimulated by CO_2 output and end-tidal CO_2 tension begins to decrease).

Measurement of Plasma AM, cAMP, and cGMP

Blood samples were immediately transferred into chilled glass tubes containing disodium EDTA (1 mg/mL) and aprotinin (500 U/mL) and centrifuged immediately at 4 C. and the plasma was frozen and stored at -80 C until assayed. Plasma AM level was measured by a specific immunoradiometric assay kit (Shionogi Pharmaceutical Co Ltd).[24] Plasma cAMP and cGMP were determined with radioimmunoassay kits (cAMP assay kit. cGMP assay kit. Yamasa Shoyu).[18]

Statistical Analysis

All data were expressed as mean ± SEM unless otherwise indicated. Changes in hemodynamic and hormonal parameters by AM inhalation were analyzed by 1-way ANOVA for repeated measures.
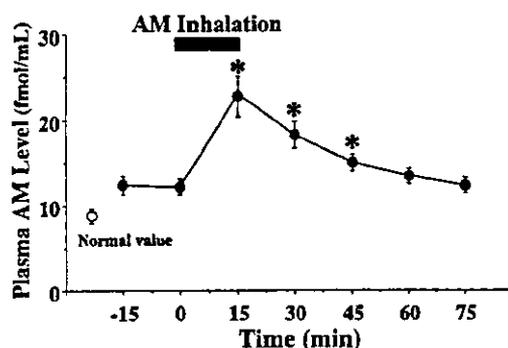
Figure 1. Changes in plasma AM level by inhalation of aerosolized AM in patients with idiopathic pulmonary arterial hypertension. Normal value indicates plasma AM level derived from 15 age-matched healthy subjects. Data are mean ± SEM. *P<0.05 vs value at time 0.

followed by Newman-Keuls test. Comparisons of exercise parameters between the 2 groups were analyzed with paired Student's *t* test. A probability value of *P*<0.05 was considered statistically significant.

Results

All patients tolerated this study protocol. One patient developed a headache, and another patient had mild arterial hypoxemia during AM inhalation. None of them experienced other adverse effects, such as systemic hypotension, infection, or arrhythmia.

Plasma AM Level After Inhalation

Baseline plasma AM level in patients with idiopathic pulmonary arterial hypertension was significantly higher than the normal value, which was determined from pooled data of 15 age-matched healthy subjects (11.9±0.8 versus 9.3±0.1 fmol/mL, *P*<0.05). Inhalation of AM significantly increased the plasma AM level to 22.9±2.1 fmol/mL immediately after inhalation (Figure 1). The half-life of plasma AM after inhalation was approximately 20 minutes, and the elevation of AM lasted for >45 minutes. Plasma cAMP level increased significantly 30 minutes after the initiation of AM inhalation (10.8±0.7 to 12.0±0.6 pmol/mL, *P*<0.05), although plasma cGMP level was not significantly altered (6.5±1.0 to 6.8±1.0 pmol/mL, *P*=NS).

Hemodynamic Effects of AM Inhalation

Inhalation of AM significantly decreased mean pulmonary arterial pressure in patients with idiopathic pulmonary arterial hypertension (54±3 to 47±3 mm Hg, *P*<0.05) without a significant decrease in mean arterial pressure (85±4 to 83±4 mm Hg, *P*=NS) (Figure 2). AM inhalation slightly but significantly increased cardiac index by 12% (2.4±0.1 to 2.7±0.2 L · min⁻¹ · m⁻², *P*<0.05). Thus, AM inhalation resulted in a 22% decrease in pulmonary vascular resistance (12.6±1.5 to 9.8±1.3 Wood units, *P*<0.05) (Figure 3). Inhaled AM did not significantly alter systemic vascular resistance. The ratio of pulmonary vascular resistance to systemic vascular resistance was decreased significantly at the end of inhalation (0.63±0.08 to 0.55±0.07, *P*<0.05). These hemodynamic effects of AM lasted for >45 minutes.
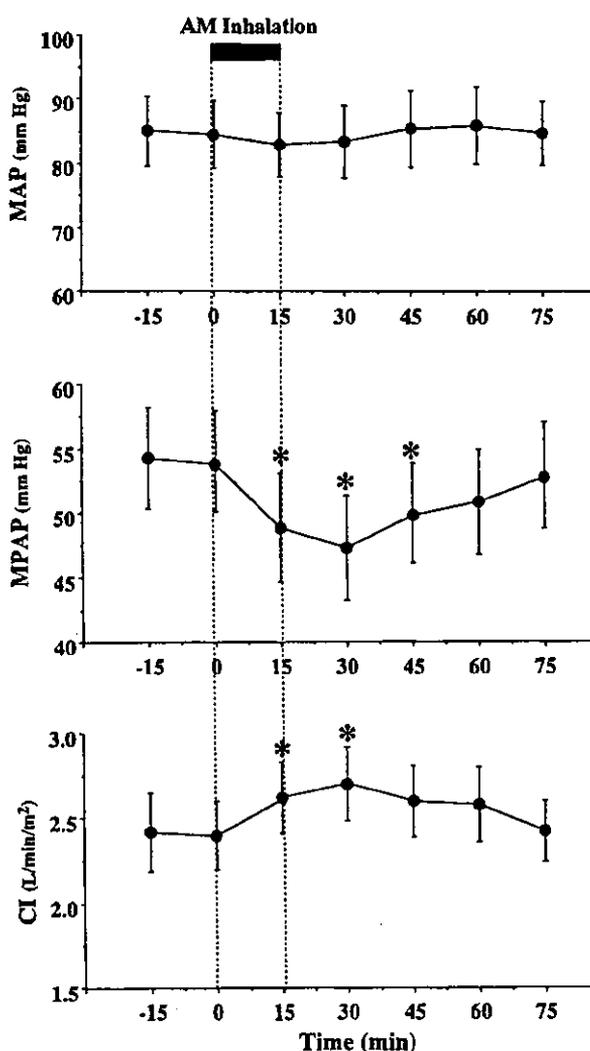

Figure 2. Changes in mean arterial pressure (MAP), mean pulmonary arterial pressure (MPAP), and cardiac index (CI) by inhalation of aerosolized AM in patients with idiopathic pulmonary arterial hypertension. Data are mean ± SEM. *P<0.05 vs value at time 0.

No significant change in heart rate, pulmonary capillary wedge pressure, or right atrial pressure was observed. There was no significant change in arterial oxygen saturation (94±3% to 93±3%).

Effects of AM Inhalation on Exercise Capacity and Ventilatory Efficiency

As the limiting symptom at the end of exercise, 6 patients reported muscle weakness and 4 reported dyspnea. There was no difference in these symptoms when exercise testing was performed with or without inhalation of AM. Inhalation of AM altered neither heart rate nor blood pressure either at rest or at peak exercise (Table 2). Inhalation of AM significantly increased peak workload (86±5 to 93±6 W, *P*<0.05) (Table 2). AM also significantly increased peak V̇o₂ (14.6±0.6 to 15.7±0.6 mL · kg⁻¹ · min⁻¹, *P*<0.05) (Figure 4). Inhalation of AM significantly increased ΔV̇o₂/ΔW ratio (6.3±0.4 to
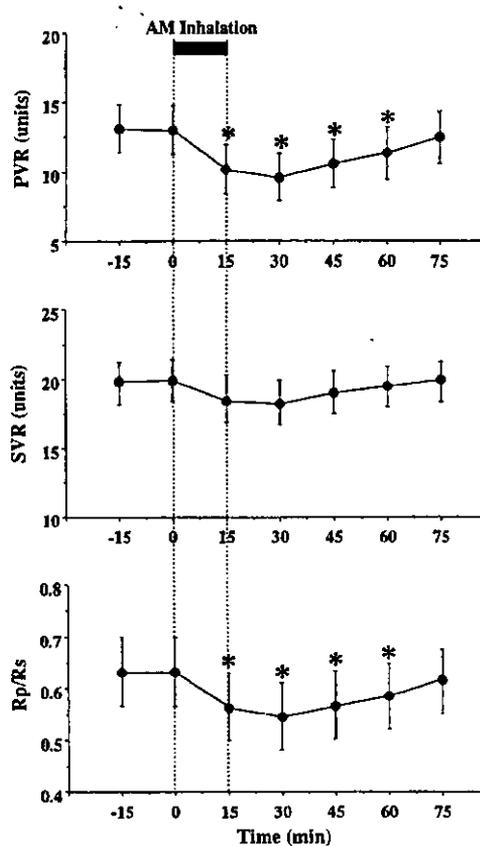
Figure 3. Changes in pulmonary vascular resistance (PVR), systemic vascular resistance (SVR), and ratio of pulmonary vascular resistance to systemic vascular resistance (Rp/Rs) by inhalation of aerosolized AM in patients with idiopathic pulmonary arterial hypertension. Data are mean±SEM. *P<0.05 vs value at time 0.

TABLE 2. Changes in Exercise Parameters by Inhalation of AM or Placebo

Variables	Placebo	AM	P
Peak workload, W	86±5	93±6	<0.05
HR, bpm			
Rest	75±5	75±3	NS
Peak	144±6	148±6	NS
MAP, mm Hg			
Rest	85 3	87±5	NS
Peak	108±5	110±6	NS
Peak Borg score (D/L)	17/18	18/18	NS
Peak $\dot{V}o_2$, mL·kg^{-1}·min^{-1}	14.6±0.6	15.7±0.6	<0.05
$\Delta\dot{V}o_2/\Delta W$ ratio, mL·min^{-1}·W^{-1}	6.3±0.4	7.0±0.5	<0.05
$\dot{V}_E$-$\dot{V}co_2$ slope	37±2	36±2	NS
Sao$_2$, %			
Rest	97±1	97±1	NS
Peak	95±1	95±1	NS

HR indicates heart rate; MAP, mean arterial pressure; Peak Borg score (D/L), Borg score at peak exercise (dyspnea/leg fatigue); Peak $\dot{V}o_2$, peak oxygen consumption; $\Delta\dot{V}o_2/\Delta W$ ratio, $\dot{V}o_2$ increase per unit workload; $\dot{V}_E$-$\dot{V}co_2$ slope, slope of regression line of relation between $\dot{V}_E$ and $\dot{V}co_2$; and Sao$_2$, arterial oxygen saturation. Data are mean±SEM.

epithelial cells attenuates chronic hypoxia-induced pulmonary hypertension in the mouse. These results raise the possibility that intratracheal delivery of a vasodilator peptide may be sufficient to alter pulmonary vascular function. In fact, in the present study, inhalation of AM significantly decreased pulmonary vascular resistance, whereas it did not alter systemic arterial pressure or systemic vascular resistance. The ratio of pulmonary vascular resistance to systemic vascular resistance was reduced significantly by AM inhalation. These results suggest that inhaled AM improves hemodynamics with pulmonary selectivity. This is consistent with earlier findings that inhaled prostacyclin or its analogue iloprost acts transepithelially with pulmonary selectivity and improves pulmonary hypertension.[20,21] Inhalation of AM slightly but significantly increased cardiac index in patients with idiopathic pulmonary arterial hypertension. Considering the strong vasodilator activity of AM in the pulmonary vasculature, the significant decrease in cardiac afterload may be responsible for increased cardiac index with

7.0±0.5 mL · min^{-1} · W^{-1}, P<0.05). AM did not significantly alter the $\dot{V}_E$-$\dot{V}co_2$ slope (Table 2). No significant changes in arterial oxygen saturation were observed either at rest or at peak exercise. In 1 patient with NYHA class IV who did not undergo cardiopulmonary exercise testing, the distance walked in 6 minutes increased from 150 to 180 m by inhalation of AM.

Discussion

In the present study, we demonstrated that inhalation of AM improved hemodynamics with pulmonary selectivity and exercise capacity in patients with idiopathic pulmonary arterial hypertension.

AM is one of the most potent endogenous vasodilators in the pulmonary vascular bed.[25–27] The vasodilatory effect is mediated by cAMP-dependent and nitric oxide-dependent mechanisms.[28,29] Endogenous AM production is enhanced in a variety of cardiovascular diseases through a compensatory mechanism.[14,30] Nonetheless, additional supplementation of AM has beneficial effects in these diseases.[18,19] These results suggest that endogenous AM level is not sufficient to improve deteriorated conditions despite the increased AM production. Interestingly, Champion et al.[31] have shown that intratracheal gene transfer of calcitonin gene-related peptide, a member of the same peptide family as AM, to bronchial
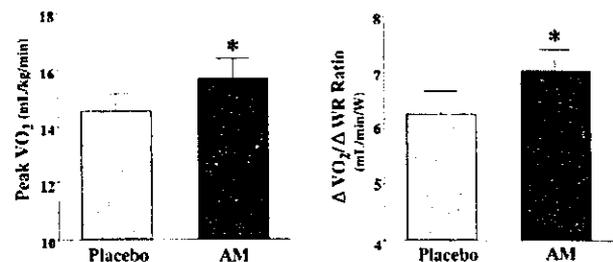

Figure 4. Changes in peak oxygen consumption (peak $\dot{V}o_2$) and ratio of change in oxygen uptake to that in work rate ($\Delta\dot{V}o_2/\Delta W$ ratio) by inhalation of aerosolized AM or placebo in patients with idiopathic pulmonary arterial hypertension. Data are mean±SEM. *P<0.05 vs placebo.

AM. Interestingly, the hemodynamic effects of inhaled AM lasted for >45 minutes. A previous study demonstrated that intravenous injection of AM produces a long-lasting vasodilator response because of its long half-life ($\approx$15 minutes).[32] The half-life of plasma AM after inhalation was longer (20 minutes). Thus, inhalation of AM may cause relatively long-lasting pulmonary vasodilator activity in patients with idiopathic pulmonary arterial hypertension. In the present study, plasma cAMP level increased after AM inhalation, suggesting that the hemodynamic effects of AM may be mediated by activation of cAMP.

Earlier studies have shown that peak $\dot{V}o_2$ during exercise is markedly lower in patients with idiopathic pulmonary arterial hypertension than in healthy subjects.[33,34] Peak $\dot{V}o_2$ is determined primarily by the maximal cardiac output during exercise and the potential for O_2 extraction by the exercising muscle.[35] Thus, the decreased peak $\dot{V}o_2$ may reflect insufficient oxygen delivery to the body during exercise, at least in part because of an inadequate increase in cardiac output under conditions of severe pulmonary hypertension. In the present study, inhalation of AM significantly increased peak $\dot{V}o_2$ in patients with pulmonary hypertension. AM also increased the $\Delta\dot{V}o_2/\Delta W$ ratio, which indicates oxygen transport per unit workload to the exercising legs. These results suggest that inhalation of AM improves exercise capacity in patients with idiopathic pulmonary arterial hypertension. It is possible that an increase in cardiac output during exercise may contribute to increases in peak $\dot{V}o_2$ and the $\Delta\dot{V}o_2/\Delta W$ ratio.

The major limitation of this pilot trial relates to the lack of a randomized, placebo-controlled group in acute hemodynamic studies, which was as result not only of invasive assessment of hemodynamics but also of the limited number of patients available. Nevertheless, cardiopulmonary exercise testing was performed in a double-blind, randomized, crossover design. Thus, it is unlikely that the hemodynamic effects of inhaled AM are attributable to the placebo effect.

Inhalation therapy may be more simple, noninvasive, and comfortable than continuous intravenous infusion therapy. An experimental study demonstrated that repeated inhalation of AM (for 30 minutes, 4 times a day) inhibited monocrotaline-induced pulmonary hypertension and markedly improved survival in rats.[36] Recently, pulmonary delivery of a dry-powder insulin has been shown to improve glycemic control without adverse pulmonary effects.[37] Although further studies are necessary to maximize the efficiency and reproducibility of pulmonary AM delivery, combining AM inhalation therapy with other modalities that have a different mode of action may have beneficial effects in patients with idiopathic pulmonary arterial hypertension.

Conclusions

These preliminary results suggest that inhalation of AM may have beneficial effects on pulmonary hemodynamics and exercise capacity in patients with idiopathic pulmonary arterial hypertension.

References

1. Rich S, Dantzker DR, Ayres SM, et al. Primary pulmonary hypertension: a national prospective study. *Ann Intern Med.* 1987;107:216–223.
2. Rich S. Primary pulmonary hypertension. *Prog Cardiovasc Dis.* 1988;31: 205–238.
3. Rubin LJ, Peter RH. Oral hydralazine therapy for primary pulmonary hypertension. *N Engl J Med.* 1980;302:69–73.
4. Rich S, Kaufmann E, Levy PS. The effect of high doses of calcium-channel blockers on survival in primary pulmonary hypertension. *N Engl J Med.* 1992;327:76–81.
5. Barst RJ, Rubin LJ, Long WA, et al. A comparison of continuous intravenous epoprostenol (prostacyclin) with conventional therapy for primary pulmonary hypertension. *N Engl J Med.* 1996;334:296–301.
6. McLaughlin VV, Genthner DE, Panella MM, et al. Reduction in pulmonary vascular resistance with long-term epoprostenol (prostacyclin) therapy in primary pulmonary hypertension. *N Engl J Med.* 1998;338:273–277.
7. Nagaya N, Uematsu M, Okano Y, et al. Effect of orally active prostacyclin analogue on survival of outpatients with primary pulmonary hypertension. *J Am Coll Cardiol.* 1999;34:1188–1192.
8. Reitz BA, Wallwork JL, Hunt SA, et al. Heart-lung transplantation: successful therapy for patients with pulmonary vascular disease. *N Engl J Med.* 1982;306:557–564.
9. Pasque MK, Trulock EP, Kaiser LD, et al. Single lung transplantation for pulmonary hypertension: three month hemodynamic follow-up. *Circulation.* 1991;84:2275–2279.
10. Kitamura K, Kangawa K, Kawamoto M, et al. Adrenomedullin: a novel hypotensive peptide isolated from human pheochromocytoma. *Biochem Biophys Res Commun.* 1993;192:553–560.
11. Ichiki Y, Kitamura K, Kangawa K, et al. Distribution and characterization of immunoreactive adrenomedullin in human tissue and plasma. *FEBS Lett.* 1994;338:6–10.
12. Sakata J, Shimokubo T, Kitamura K, et al. Distribution and characterization of immunoreactive rat adrenomedullin in tissue and plasma. *FEBS Lett.* 1994;352:105–108.
13. Owji AA, Smith DM, Coppock HA, et al. An abundant and specific binding site for the novel vasodilator adrenomedullin in the rat. *Endocrinology.* 1995;136:2127–2134.
14. Kakishita M, Nishikimi T, Okano Y, et al. Increased plasma levels of adrenomedullin in patients with pulmonary hypertension. *Clin Sci.* 1999;96: 33–39.
15. Yoshibayashi M, Kamiya T, Kitamura K, et al. Plasma levels of adrenomedullin in primary and secondary pulmonary hypertension in patients < 20 years of age. *Am J Cardiol.* 1997;79:1556–1558.
16. Horio T, Kohno M, Kano H, et al. Adrenomedullin as a novel antimigration factor of vascular smooth muscle cells. *Circ Res.* 1995;77:660–664.
17. Kano H, Kohno M, Yasunari K, et al. Adrenomedullin as a novel antiproliferative factor of vascular smooth muscle cells. *J Hypertens.* 1996;14: 209–213.
18. Nagaya N, Satoh T, Nishikimi T, et al. Hemodynamic, renal, and hormonal effects of adrenomedullin infusion in patients with congestive heart failure. *Circulation.* 2000;101:498–503.
19. Nagaya N, Nishikimi T, Uematsu M, et al. Haemodynamic and hormonal effects of adrenomedullin in patients with pulmonary hypertension. *Heart.* 2000;84:653–658.
20. Walmrath D, Schneider T, Pilch J, et al. Aerosolized prostacyclin reduces pulmonary artery pressure and improves gas exchange in the adult respiratory distress syndrome (ARDS). *Lancet.* 1993;342:961–962.
21. Hoeper MM, Schwarze M, Ehlerding S, et al. Long-term treatment of primary pulmonary hypertension with aerosolized iloprost, a prostacyclin analogue. *N Engl J Med.* 2000;342:1866–1870.
22. Rich S, Seidlitz M, Dodin E, et al. The short-term effects of digoxin in patients with right ventricular dysfunction from pulmonary hypertension. *Chest.* 1998;114:787–792.
23. Miyamoto S, Nagaya N, Satoh T, et al. Clinical correlates and prognostic significance of six-minute walk test in patients with primary pulmonary

hypertension: comparison with cardiopulmonary exercise testing. *Am J Respir Crit Care Med*. 2000;161:487–492.

24. Ohta H, Tsuji T, Asai S, et al. A simple immunoradiometric assay for measuring the entire molecules of adrenomedullin in human plasma. *Clin Chim Acta*. 1999;287:131–143.

25. Lippton H, Chang JK, Hao Q, et al. Adrenomedullin dilates the pulmonary vascular bed in vivo. *J Appl Physiol*. 1994;76:2154–2156.

26. Heaton J, Lin B, Chang JK, et al. Pulmonary vasodilation to adrenomedullin: a novel peptide in humans. *Am J Physiol*. 1995;268:H2211–H2215.

27. Nossaman BD, Feng CJ, Kaye AD, et al. Pulmonary vasodilator responses to adrenomedullin are reduced by NOS inhibitors in rats but not in cats. *Am J Physiol*. 1996;270:L782–L789.

28. Ishizaka Y, Ishizaka Y, Tanaka M, et al. Adrenomedullin stimulates cyclic AMP formation in rat vascular smooth muscle cells. *Biochem Biophys Res Commun* 1994;200:642–646.

29. Nakamura M, Yoshida H, Makita S, et al. Potent and long-lasting vasodilatory effects of adrenomedullin in humans: comparisons between normal subjects and patients with chronic heart failure. *Circulation*. 1997;95: 1214–1221.

30. Nagaya N, Nishikimi T, Yoshihara F, et al. Cardiac adrenomedullin gene expression and peptide accumulation after acute myocardial infarction in rats. *Am J Physiol*. 2000;278:R1019–R1026.

31. Champion HC, Bivalacqua TJ, Toyoda K, et al. In vivo gene transfer of prepro-calcitonin gene-related peptide to the lung attenuates chronic hypoxia-induced pulmonary hypertension in the mouse. *Circulation*. 2000;101: 931–937.

32. Ishiyama Y, Kitamura K, Ichiki Y, et al. Haemodynamic responses to rat adrenomedullin in anaesthetized spontaneously hypertensive rats. *Clin Exp Pharmacol Physiol*. 1995;22:614–618.

33. D'Alonzo GE, Gianotti LA, Pohil RL, et al. Comparison of progressive exercise performance of normal subjects and patients with primary pulmonary hypertension. *Chest*. 1987;92:57–62.

34. Wensel R, Opitz CF, Anker SD, et al. Assessment of survival in patients with primary pulmonary hypertension: importance of cardiopulmonary exercise testing. *Circulation*. 2002;106:319–324.

35. Anderson P, Saltin B. Maximal perfusion of skeletal muscle in man. *J Appl Physiol*. 1985;366:233–249.

36. Nagaya N, Okumura H, Uematsu M, et al. Repeated inhalation of adrenomedullin ameliorates pulmonary hypertension and survival in monocrotaline rats. *Am J Physiol Heart Circ Physiol*. 2003;285:H2125–H2131.

37. Skyler JS, Cefalu WT, Kourides IA, et al. Efficacy of inhaled human insulin in type 1 diabetes mellitus: a randomised proof-of-concept study. *Lancet*. 2001;357:331–335.

Adrenomedullin Gene Transfer Induces Therapeutic Angiogenesis in a Rabbit Model of Chronic Hind Limb Ischemia

Benefits of a Novel Nonviral Vector, Gelatin

Noriyuki Tokunaga, MD; Noritoshi Nagaya, MD; Mikiyasu Shirai, MD; Etsuro Tanaka, MD;
Hatsue Ishibashi-Ueda, MD; Mariko Harada-Shiba, MD; Munetake Kanda, MD; Takefumi Ito, MD;
Wataru Shimizu, MD; Yasuhiko Tabata, PhD; Masaaki Uematsu, MD; Kazuhiro Nishigami, MD;
Shunji Sano, MD; Kenji Kangawa, PhD; Hidezo Mori, MD

Background—Earlier studies have shown that adrenomedullin (AM), a potent vasodilator peptide, has a variety of cardiovascular effects. However, whether AM has angiogenic potential remains unknown. This study investigated whether AM gene transfer induces therapeutic angiogenesis in chronic hind limb ischemia.

Methods and Results—Ischemia was induced in the hind limb of 21 Japanese White rabbits. Positively charged biodegradable gelatin was used to produce ionically linked DNA-gelatin complexes that could delay DNA degradation. Human AM DNA (naked AM group), AM DNA-gelatin complex (AM-gelatin group), or gelatin alone (control group) was injected into the ischemic thigh muscles. Four weeks after gene transfer, significant improvements in collateral formation and hind limb perfusion were observed in the naked AM group and AM-gelatin group compared with the control group (calf blood pressure ratio: 0.60±0.02, 0.72±0.03, 0.42±0.06, respectively). Interestingly, hind limb perfusion and capillary density of ischemic muscles were highest in the AM-gelatin group, which revealed the highest content of AM in the muscles among the three groups. As a result, necrosis of lower hind limb and thigh muscles was minimal in the AM-gelatin group.

Conclusions—AM gene transfer induced therapeutic angiogenesis in a rabbit model of chronic hind limb ischemia. Furthermore, the use of biodegradable gelatin as a nonviral vector augmented AM expression and thereby enhanced the therapeutic effects of AM gene transfer. Thus, gelatin-mediated AM gene transfer may be a new therapeutic strategy for the treatment of peripheral vascular diseases. (***Circulation.*** 2004;109:526-531.)

Key Words: peripheral vascular disease ■ angiogenesis ■ gene therapy ■ ischemia

A drenomedullin (AM) is a potent vasodilator peptide that was originally isolated from human pheochromocytoma.[1] AM and its receptor are expressed mainly in vascular endothelial cells and vascular smooth muscle cells.[2–4] AM not only induces vasorelaxation but also regulates growth and death of these vascular cells.[5–10] These findings suggest that AM plays an important role in maintaining vascular homeostasis in an autocrine and/or paracrine manner.

A recent study has shown that vascular abnormalities are present in homozygous AM knockout mice, suggesting

that AM is indispensable for vascular morphogenesis.[11–13] More recently, AM has been shown to activate the PI3K/Akt-dependent pathway in vascular endothelial cells, which is considered to regulate multiple critical steps in angiogenesis, including endothelial cell survival, proliferation, migration, and capillary-like structure formation.[7,14] These results raise the possibility that AM plays a role in modulating vasculogenesis and angiogenesis. However, whether AM induces therapeutic angiogenesis remains unknown.
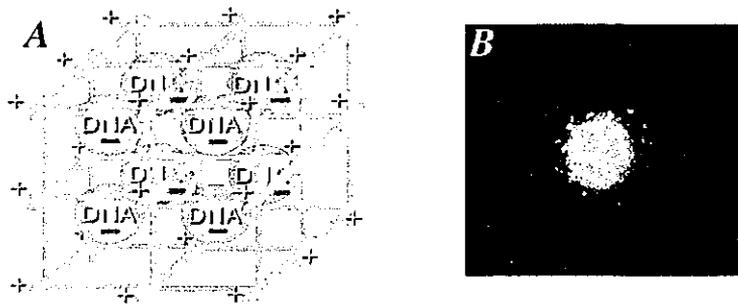
Figure 1. A, Schema of DNA-gelatin complex. Bio-degradable gelatin can hold negatively charged plasmid DNA in its positively charged lattice structure. B, RITC-labeled AM DNA particles were incorporated into gelatin.

We prepared biodegradable gelatin that could hold negatively charged protein or plasmid DNA in its positively charged lattice structure.[15,16] Biodegradable gelatin has been widely used as a carrier of protein because of its capacity to delay protein degradation.[15] Similarly, ionically linked DNA-gelatin complexes can delay gene degradation.[16] These findings raise the possibility that gelatin may serve as a nonviral vector for gene therapy.

Thus, the purposes of this study were (1) to investigate whether AM gene transfer induces therapeutic angiogenesis in a rabbit model of chronic hind limb ischemia and (2) to examine whether the use of biodegradable gelatin as a vector augments AM expression and thereby enhances the therapeutic effects of AM gene transfer.

Methods

Animal Model

All protocols were performed in accordance with the guidelines of the Animal Care Ethics Committee of the National Cardiovascular Center Research Institute. Twenty-one male Japanese White rabbits (body weight, 2.9±0.1 kg; Japan Animal Co, Osaka, Japan) were used for physiological and morphological assessment. In addition, 30 rabbits were used for radioimmunoassay, immunohistochemical examination, and Western blot analysis. After anesthetization with pentobarbital sodium (30 to 35 mg/kg), a longitudinal incision was made in the left thigh, extending inferiorly from the inguinal ligament to a point just proximal to the patella. Hind limb ischemia was induced by ligation of the distal left external iliac artery and complete resection of the left femoral artery, as described previously.[17]

Construction of Plasmid DNA

To construct the expression vector for human AM, the EcoRI/XhoI fragment of the full-length human AM cDNA was ligated into the EcoRI/XhoI fragment of the pcDNA1.1-CMV expression plasmid (Invitrogen). To verify that the pcDNA1.1-CMV vector encoding AM cDNA produces a biologically active AM protein, the expression vector was transfected into 293 cells, and AM activity in the transfected cells was measured by high-performance liquid chromatography and radioimmunoassay. The pcDNA1.1-CMV vector encoding β-galactosidase (LacZ) cDNA was used as a control DNA.

Preparation of AM DNA-Gelatin Complex

Biodegradable gelatin was prepared from pig skin. The gelatin was characterized by a spheroid shape with a diameter of approximately 30 μm, water content of 95%, and an isoelectric point (pI) of 9 after swelling in water.[15,16] Gelatin can hold negatively charged protein or plasmid DNA in its positively charged lattice structure (Figure 1A). Dried gelatin (4 mg, pI 9) was added to human AM DNA solution (500 μg/100 μl) in phosphate-buffered saline, pH 7.4). After mixture of DNA and gelatin, DNA-gelatin complexes were incubated at 37 C for 2 hours.

To visualize incorporation of DNA into gelatin, AM plasmid DNA was labeled with rhodamine B isothiocyanate (RITC), as reported previously.[16] In brief, the coupling reaction of RITC to plasmid DNA was carried out by mixing the two substances in 0.2 mol/L sodium carbonate-buffered solution (pH 9.7), followed by gel filtration with a PD 10 column (Amersham-Pharmacia). RITC-labeled AM DNA was incorporated into positively charged gelatin (Figure 1B).

Study Protocol

Ten days after the induction of hind limb ischemia (day 10), AM DNA (naked AM group, n=7), AM DNA-gelatin complex (AM-gelatin group, n=7), or gelatin alone (control group, n=7) was administered intramuscularly into 3 different sites in the ischemic adductor muscle and 2 different sites in the semimembranous muscle. In addition, LacZ DNA-gelatin complex served as a control DNA (LacZ-gelatin group, n=5). The amount of plasmid was 500 μg (1 mL) and that of gelatin was 4 mg. Morphological and angiographic analyses and measurements of calf blood pressure and laser Doppler flow were performed 4 weeks after gene transfer (day 38). After completion of these measurements, the adductor, semimembranous, and gastrocnemius muscles were weighed in each hind limb.[18] The muscle weight ratio was calculated for each muscle as follows: muscle weight ratio=muscle weight in ischemic hind limb muscle weight in nonischemic hind limb. Specimens of the adductor muscle of the ischemic hind limb were obtained for histological examination.

Measurement of Calf Blood Pressure

Calf blood pressure was measured on days 10 and 38 in both hind limbs with a Doppler flowmeter (Hayashi Denki Co, Ltd) and a 25-mm-wide cuff. The pulse of the posterior tibial artery was identified with the use of a Doppler probe, and the systolic blood pressure in both hind limbs was determined by standard techniques. The calf blood pressure ratio was defined for each rabbit as the ratio of systolic pressure of the ischemic hind limb to that of the normal hind limb.[17]

Laser Doppler Blood Perfusion Analysis

Blood flow of the ischemic hind limb was measured with the use of a laser Doppler blood perfusion image system (moorLDI, Moor Instruments) on day 38.

Angiographic Analysis

Development of collateral arteries was evaluated by angiography on days 0 and 38. A 4F catheter was placed in the left internal iliac artery through the common carotid artery, and 3 mL contrast medium (Iopamiron 300, SCHERING) was injected with an automated angiography injector at a rate of 2.5 mL/s. Quantitative angiographic analysis of collateral vessel development in the ischemic hind limb was performed with the use of a 5-mm² grid overlay, as described previously.[17] The angiographic score was calculated for each film as the ratio of grid intersections crossed by opacified arteries divided by the total number of grid intersections in the ischemic medial thigh. The angiographic score was determined by 2 blinded observers.

Morphological and Histological Examination

The degree of lower hind limb necrosis and thigh muscle necrosis was macroscopically evaluated on graded morphological scales (grade 1 to 3) for peripheral tissue damage and muscle necrosis area of the adductor, semimembranous, and medial large muscles. Capillary density of the ischemic hind limb was evaluated by alkaline phosphatase staining, as reported previously.[17] A total of 10 different fields from three different sections were randomly selected, and the number of capillaries was counted under a ×40 objective. Capillary density was expressed as the mean number of capillaries per square millimeter. The number of myofibers in each field was also examined and the capillary/muscle fiber ratio calculated.

Radioimmunoassay for Human AM

Human AM production was examined 1, 2, and 4 weeks after gene transfer in the naked AM group, AM-gelatin group, and control group (n=5 each). The muscles were harvested for radioimmunoassay and immunohistochemical examination. Immunoreactive human AM level in rabbit muscles was determined by immunoradiometric assay with the use of a specific kit (Shionogi Co, Ltd).[18] Tissue content of vascular endothelial growth factor (VEGF) was examined by ELISA kit (R&D systems).

Immunohistochemistry for Human AM, Ki67 Antigen, and Phosphorylated Akt

Immunohistochemical studies were performed on formalin-fixed, paraffin-embedded 4-μm sections of ischemic thigh muscles 7 days after gene transfer. To elucidate AM expression after gene therapy, immunohistochemistry for human AM was performed with the use of a monoclonal antibody recognizing AM-(12-25) (1:100), as reported previously.[20] To evaluate the proliferative potential of AM, tissue sections were stained for Ki67, a marker for cell proliferation, with the use of monoclonal anti-Ki67 antibody (1:100) (DAKO). AM has recently been shown to promote proliferation of vascular endothelial cells at least in part through the PI3k-Akt pathway.[21] Thus, immunohistochemistry for phosphorylated Akt was performed with mouse monoclonal anti-phosphorylated Akt antibody (1:100) (Cell Signaling Technology).

Western Blot Analysis

To identify Akt phosphorylation in ischemic muscles after AM gene transfer, Western blotting was performed with the use of a commercially available kit (PhosphoPlus Akt [Ser473] Antibody Kit, Cell Signaling Technology). Ischemic muscles in the 3 groups were obtained 7 days after AM gene transfer. These samples were homogenized on ice in 0.1% Tween 20 homogenization buffer with a protease inhibitor (Complete, Roche). After centrifugation for 20 minutes at 4°C, the supernatant was used for Western blot analysis. The 50 μg of protein was transferred into sample buffer, loaded on 7.5% SDS-polyacrylamide gel, and blotted onto nitrocellulose membrane through the use of a wet blotting system. After blocking for 60 minutes, the membranes were incubated with primary antibodies (1:500) at 4°C overnight. The membranes were then incubated with secondary antibodies, which were conjugated with horseradish peroxidase (Cell Signaling Technology), at a final dilution of 1:2000. Signals were detected through the use of LumiGLO chemiluminescence reagents (Cell Signaling Technology).

Statistical Analysis

All results are expressed as mean±SEM. Statistical significance was evaluated by 1-way ANOVA followed by Fisher's analysis, Scheffe's F analysis, or Kruskal-Wallis test. A value of $P<0.05$ was considered statistically significant.

Results

Physiological and Morphological Assessment

Complete resection of the left femoral artery resulted in a similar decrease in calf blood pressure ratio among the 3
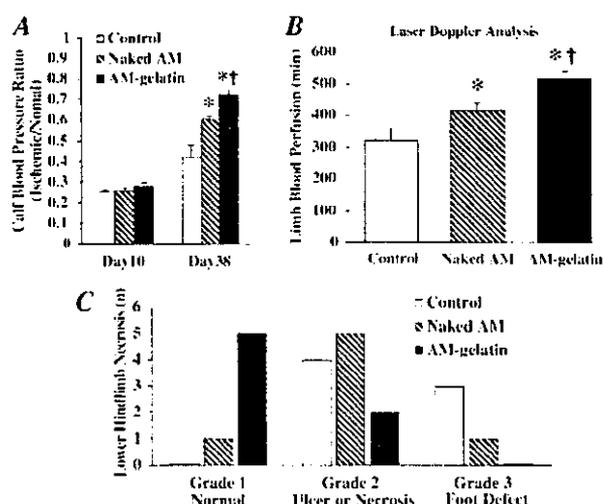

Figure 2. A, Calf blood pressure ratio (ischemic/normal hind limb) before (on day 10) and after (on day 38) gene transfer. B, Measurement of laser Doppler flow on day 38. Data are mean ± SEM. $^*P<0.05$ vs control group; $\dagger P<0.05$ vs naked AM group. C, Number of cases of each grade of lower hind limb necrosis on day 38. Lower hind limb necrosis was minimal in the AM-gelatin group. Number of necrosis or foot defect is statistically significant among the 3 groups ($P<0.05$ by Kruskal-Wallis test).

groups before the initiation of therapy (day 10) (Figure 2A). However, the calf blood pressure ratio on day 38 was highest in the AM-gelatin groups, followed by the naked AM group and subsequently the control group. The laser Doppler flow in hind limb was highest in the AM-gelatin group, followed by the naked AM group and the control group (Figure 2B). The calf blood pressure ratio and laser Doppler flow 4 weeks after gene transfer did not significantly differ between the control group and 1 ae Z-gelatin group. Lower hind limb necrosis was minimal in the AM-gelatin group, followed by the naked AM group and the control group (Figure 2C). Thigh muscle necrosis was also minimal in the AM-gelatin group. Similarly, the muscle weight ratio (ischemic/normal) on day 38 was highest in the AM-gelatin group (Table). Neither mean arterial pressure nor heart rate significantly differed among the 3 groups.

Angiographic Analysis

Angiograms 4 weeks after gene transfer (day 38) showed the development of collateral arteries in the naked AM and

Physiological Characteristics

	Control	Naked AM	AM-Gelatin
No. of rabbits	7	7	7
Body weight, kg	2.46 ± 0.06	2.65 ± 0.10	3.16 ± 0.09
MAP, mm Hg	112 ± 3	114 ± 3	116 ± 2
HR, beats/min	269 ± 12	253 ± 5	262 ± 7
Muscle weight ratio	0.71 ± 0.03	0.84 ± 0.02*	0.95 ± 0.02*†

MAP indicates mean arterial pressure; HR, heart rate; and muscle weight ratio, ratio of muscle weight in ischemic hind limb to that in nonischemic hind limb. Data are mean ± SEM.

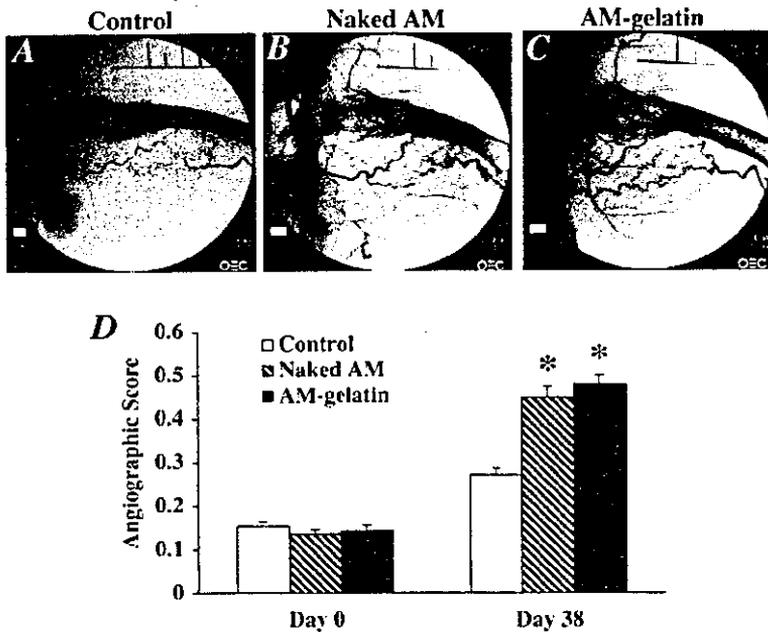$^*P<0.01$ vs control group; $\dagger P<0.05$ vs naked AM group.

Figure 3. Representative angiograms of control group (A), naked AM group (B), and AM-gelatin group (C) on day 38. Collateral arteries were well developed in the naked AM and AM-gelatin groups. D, Angiographic score on days 0 and 38 in each group. Angiographic score on day 38 was significantly higher in the naked AM and AM-gelatin groups than in the control group. Data are mean±SEM. *P<0.001 versus control group.

AM-gelatin groups compared with that in the control group (Figure 3, A through C). Quantitative analysis of collateral vessels demonstrated that the angiographic score in both the naked AM and AM-gelatin groups was significantly higher than that in the control group (Figure 3D). Angiographic score did not significantly differ between the control group and Lac Z-gelatin group.

To examine the development of collateral vessels in an earlier stage, other rabbits (n=4 each) were examined 2 weeks after gene transfer (day 24). Angiograms showed significant collateral development in the naked AM and AM-gelatin groups compared with that in the control group.

Histological Examination

Alkaline phosphatase staining of ischemic hind limb muscle showed marked augmentation of neovascularization in both the naked AM and AM-gelatin groups compared with the control group (Figure 4, A through C). Quantitative analysis demonstrated that capillary density of the ischemic adductor muscle was highest in the AM-gelatin group (Figure 4D). Analysis of the capillary/muscle fiber ratio yielded similar

results. Seven days after gene transfer, intense immunostaining for Ki67 was observed in vascular endothelial cells of the naked AM and the AM-gelatin groups (Figure 4, E through G).

AM Expression and Akt Phosphorylation After Gene Transfer

Seven days after gene transfer, modest immunostaining for human AM was observed in the naked AM group, whereas AM immunoreactivity was intense surrounding the gelatin in the AM-gelatin group (Figure 5, A through C). Tissue content of human AM was significantly increased both in the naked AM and the AM-gelatin groups 7 days after gene transfer (Figure 5D). The AM level in the AM-gelatin group was significantly higher that in the naked AM group. Two weeks after gene transfer, AM overexpression was observed only in the AM-gelatin group. The expression of endogenous VEGF and its receptors (Flt-1 and Flk-1) did not differ among the 3 groups (data not shown). Western blot analysis revealed that phosphorylated Akt in ischemic muscles was increased in both the naked AM and AM-gelatin groups 7 days after gene transfer (Figure 5E). Intense immunostaining for phosphory-
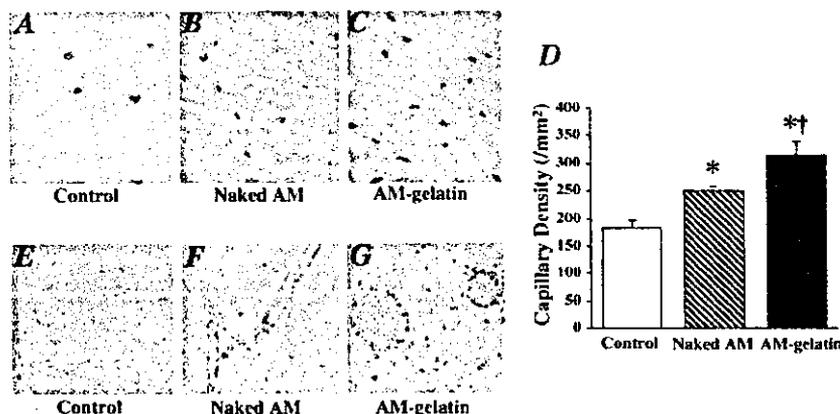

Figure 4. A through C, Representative examples of alkaline phosphatase staining in ischemic hind limb muscles. Magnification ×200. D, Quantitative analysis of capillary density in ischemic hind limb muscles. Data are mean± SEM. *P<0.05 vs control group; †P<0.05 vs naked AM group. E through G, Immunohistochemical analysis of Ki67 antigen, a marker for cell proliferation. Magnification ×400.
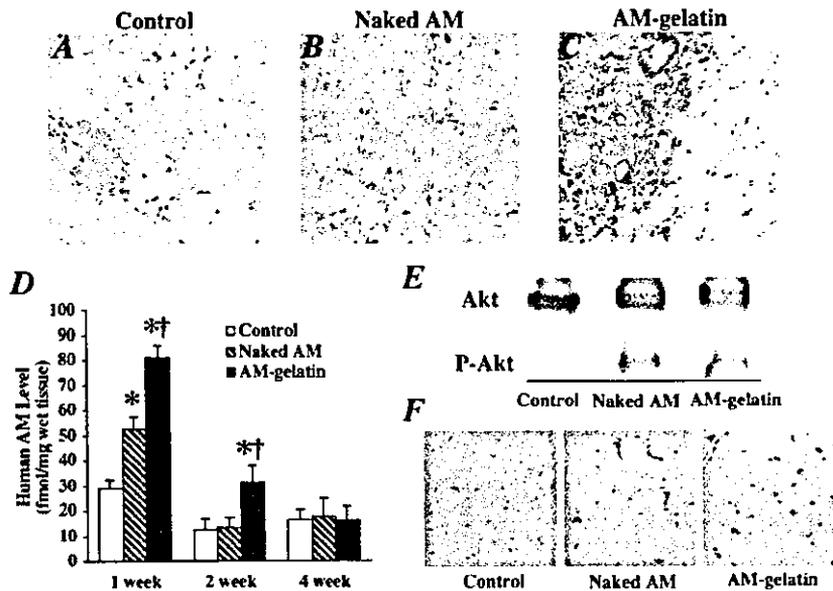
Figure 5. A through C, Immunohisto-chemistry for human AM 7 days after gene transfer. Intense immunostaining was observed surrounding gelatin in the AM-gelatin group. Magnification ×200. D, Time course of AM production in ischemic muscles after gene transfer. Data are mean±SEM. *P<0.01 vs control group; †P<0.01 vs naked AM group. E, Western blot analysis for Akt phosphorylation in muscles. F, Immunohistochemical staining for phosphorylated Akt 7 days after gene transfer. Phosphorylated Akt was distributed at least in endothelial cells. Magnification ×400.

lated Akt was observed at least in endothelial cells of the Naked AM and the AM-gelatin groups (Figure 5F).

Discussion

We demonstrated that (1) AM gene transfer induced hemodynamic and angiographic improvements in association with an increase in capillary density in a rabbit model of chronic hind limb ischemia. We also demonstrated that (2) administration of AM DNA-gelatin complexes markedly augmented AM expression and thereby enhanced the therapeutic effects of AM gene transfer.

AM has a variety of effects on the vasculature that include vasodilation,[1-7] inhibition of endothelial cell apoptosis,[8,9] and regulation of smooth muscle cell proliferation.[10] However, whether AM has angiogenic potential has remained unknown. In the present study, intramuscular administration of naked AM DNA augmented AM production in skeletal muscles, as indicated by increased tissue content and significant immunostaining of AM. As a result, AM gene transfer increased hind limb perfusion and ameliorated lower hind limb and thigh muscle necrosis in a rabbit model of hind limb ischemia. AM gene transfer may protect the ischemic hind limb partly by improving the blood flow in the ischemic hind limb because AM is originally identified as a potent vasodilating peptide.[1] Nevertheless, angiographic collateral development and high capillary density were observed in ischemic muscles after AM gene transfer. Ki67, a marker for cell proliferation, was detected in endothelial cells of microvessels after AM gene transfer. These results suggest that AM overproduction resulting from gene transfer may induce angiogenesis in a rabbit model of hind limb ischemia. Recent studies using AM gene knockout mice have shown that AM is essential for development of the vasculature during embryogenesis.[11-13] These studies support our results that AM may be an angiogenic factor. VEGF is known to induce angiogenesis and to regulate endothelial cell survival through the phosphatidylinositol 3-kinase (PI3K)/Akt pathway.[22] Thus, the PI3K/Akt pathway is considered to regulate multiple critical steps in angiogenesis, including endothelial cell survival, proliferation, migration, and capillary-like structure formation.[14] A recent study has reported that AM promotes proliferation and migration of human umbilical vein endothelial cells at least in part through the PI3K/Akt pathway.[21] The present study demonstrated that phosphorylated Akt is increased at least in endothelial cells after AM gene transfer. AM gene transfer did not influence endogenous VEGF and its receptors. Taken together, it is interesting to speculate that AM may directly induce angiogenesis through the PI3K/Akt pathway.

In the present study, we used positively charged biodegradable gelatin as a nonviral vector. We have shown that basic fibroblast growth factor (bFGF) is ionically linked with gelatin, which enhances the angiogenic effects of bFGF by delaying protein degradation.[15] Thus, biodegradable gelatin has been used as a carrier of protein. However, little information is available regarding the therapeutic potential of gelatin as a nonviral vector for gene transfer. In the present study, we demonstrated that RITC-labeled AM DNA was incorporated into positively charged gelatin. In addition, intramuscular administration of AM DNA-gelatin complexes strongly enhanced AM production compared with that of naked AM DNA. These results suggest that biodegradable gelatin may serve as a vector for gene transfer. In fact, AM DNA-gelatin complexes induced more potent angiogenic effects in a rabbit model of hind limb ischemia than naked AM DNA, as evidenced by significant increases in histological capillary density, calf blood pressure ratio, laser Doppler flow, and muscle weight ratio and a decrease in necrosis of lower hind limb and thigh muscles. These results suggest that the use of biodegradable gelatin as a nonviral vector augments AM expression and enhances AM-induced angiogenic effects. The angiogenic effects of AM-gelatin complexes were comparable to those of bFGF-gelatin complexes (data not shown). AM DNA-gelatin complexes were distributed mainly in connective tissues. We have recently demonstrated that gelatin-DNA complex is readily phagocytosed by mac-